Pharmaceutical Research, Vol. 23, No. 10, October 2006 (© 2006)
DOI: 10.1007/s11095-006-9051-0

Research Paper

Solute Crystallization in Frozen Systems–Use of Synchrotron Radiation to Improve Sensitivity

Dushyant B. Varshney,[1,2] Satyendra Kumar,[3] Evgenyi Y. Shalaev,[4] Shin-Woong Kang,[3] Larry A. Gatlin,[4] and Raj Suryanarayanan[1,5]

Received January 24, 2006; accepted May 5, 2006; published online August 23, 2006

Purpose. To demonstrate the sensitivity of low temperature synchrotron X-ray diffractometry (SXRD) for detecting solute crystallization in frozen sodium phosphate buffer solutions. To determine the effect of annealing on solute crystallization in frozen solutions.
Materials and Methods. Sodium phosphate buffer solutions, at initial buffer concentrations ranging from 1 to 100 mM (pH 7.4) were cooled to −50°C. The crystallization of disodium hydrogen phosphate dodecahydrate ($Na_2HPO_4 \cdot 12H_2O$) was monitored using a laboratory as well as a synchrotron source. At selected concentrations, the effect of annealing (at −20°C) was investigated.
Results. With the laboratory source, solute crystallization, based on the appearance of one diagnostic peak with a *d*-spacing of 5.4 Å, was evident only when the initial buffer concentration was at least 50 mM. In contrast, using SXRD, crystallization was detected at initial buffer concentrations down to 1 mM. In addition, the use of a high-resolution 2D detector enabled the visualization of numerous diffraction rings of the crystalline solute. At both 10 and 100 mM buffer concentration, there was no increase in solute crystallization due to annealing.
Conclusion. By using synchrotron radiation, solute crystallization was detected with substantially increased sensitivity, making the technique useful for freeze-drying cycles of practical and commercial importance. Since numerous peaks of the crystalline solute appeared, the technique has potential utility in complex, multi-component systems.

KEY WORDS: annealing; buffer salt; disodium hydrogen phosphate dodecahydrate; solute crystallization; synchrotron XRD.

INTRODUCTION

Freeze-drying (lyophilization) is extensively used for the dry state stabilization of thermolabile therapeutic agents. Freeze-dried pharmaceutical formulations are typically multi-component systems, and contain in addition to the active pharmaceutical ingredient (API), excipients such as bulking agents, lyoprotectants and buffers. The physical form of the API and the excipients in the final lyophile will influence the product stability (chemical as well as physical) and performance (reconstitution time) (1–5).

In case of buffering agents, selective crystallization of a buffering component can lead to significant pH shifts in the freeze-concentrated phase. For example, in phosphate buffer system, the crystallization of disodium hydrogen phosphate dodecahydrate (DHPD) in frozen solutions, and its impact on the stability of formulation components has been extensively investigated (6–11). Specifically, in protein formulations, the loss in API activity was attributed to the pH shift (up to 3 units) during the initial stage of freeze-cooling (8,9). Moreover, other buffers such as succinates and tartarates have also demonstrated the potential to crystallize (6). Typically the buffer concentration is very low in a prelyo solution and the detection of its crystallization in frozen systems can be an analytical challenge. The problem can be exacerbated not only by the presence of crystalline ice, but also due to other formulation components (4,12–14).

The crystallization behavior in the phosphate buffer system, consisting of monosodium dihydrogen phosphate and disodium hydrogen phosphate, has been extensively investigated. This has been accomplished either by direct methods, for example by measuring the cation and anion concentrations by flame photometry or by low temperature X-ray diffractometry (XRD), or indirect approaches, for example, based on the shift in the pH of the freeze-concentrate (15–25). The pioneering work of van der Berg *et al*. provided insights into the selective crystallization of disodium hydrogen phosphate as DHPD in close-to-equilibrium conditions (15–17). Gomez *et al.* developed an elegant method, utilizing a low-temperature pH electrode, to measure the pH shifts during the freezing stage under far-from-equilibrium conditions (18,19).

[1] Department of Pharmaceutics, College of Pharmacy, University of Minnesota, Minneapolis, Minnesota 55455, USA.
[2] Present address: Eli Lilly and Company, Lilly Corporate Center, Indianapolis, Indiana 46285, USA.
[3] Department of Physics, Kent State University, Kent, Ohio 44242, USA.
[4] Pfizer Groton Laboratories, Groton, Connecticut 06340, USA.
[5] To whom correspondence should be addressed. (e-mail: surya001@umn.edu)

Direct techniques for observing solute crystallization suffer from low sensitivity. For example, based on both XRD and DSC, crystallization could not be detected at initial buffer concentrations <190 mM. Consequently, it was difficult to investigate directly the crystallization of DHPD, at concentrations and processing conditions that are used in commercial freeze-drying. The indirect techniques, wherein salt crystallization is *inferred* and not directly detected, tend to be much more sensitive. The use of a low temperature pH electrode indicated DHPD crystallization at initial buffer concentration down to 8 mM. However, the pH electrode could only be used at temperatures $\geq -17°C$. Thus, the utility of the technique may be limited when dealing with freeze-drying cycles wherein the system is typically cooled to −40°C and subjected to reduced pressure.

The poor sensitivity of the laboratory based XRD method could be attributed to the low flux of the X-ray source, and the use of a point detector (24,25). These limitations could be overcome with the use of highly collimated and brilliant synchrotron radiation, coupled with a high-resolution 2D detector. Although synchrotron based X-ray diffractometry (SXRD) has been extensively used to characterize pharmaceutical systems including single crystal XRD studies, *in situ* monitoring of crystallization, solution mediated polymorphic transformation, and quantification of crystallinity in a substantially amorphous matrix (26–30), SXRD has not been applied to study freezing and freeze-drying processes. In addition to the increased sensitivity, very rapid data collection is possible (<1 s) enabling time-resolved studies.

The unique capabilities of SXRD could be extended to detect solute crystallization in frozen systems. Additionally, SXRD offers numerous advantages. (a) Capability to monitor phase transitions, *in situ*, during the entire freeze-drying cycle. (b) Potential for obtaining quantitative information based on the intensity of the analyte peak(s). By collecting the entire diffraction data (the Debye rings), errors in net intensity measurement due to preferred orientation can be minimized. (c) Determine, in real time, the effect of processing. For example, the kinetics of solute crystallization as a function of annealing time and temperature. (d) Quantification of analyte crystallinity in complex, multi-component systems.

The objective of this investigation was to demonstrate the superior sensitivity of SXRD, compared with laboratory based XRD, for the detection of solute crystallization in frozen solutions. A pharmaceutically relevant phosphate buffer system (*disodium hydrogen phosphate + monosodium dihydrogen phosphate; pH 7.4*) was selected, wherein the crystallization of $Na_2HPO_4 \cdot 12H_2O$ (DHPD) was monitored. Our second objective was to determine the effect of annealing on the extent of solute crystallization.

The detection of DHPD was unambiguous, based on several unique peaks, and was accomplished under far-from-equilibrium conditions. To our knowledge, this is the first report of direct detection of DHPD crystallization from frozen buffer solutions, wherein the initial buffer concentration was as low as 1 mM. In light of the substantially improved sensitivity, this direct technique becomes relevant for freeze-drying cycles of practical interest, and may be extended to study other buffer systems. Based on the intensities of numerous characteristic peaks of DHPD, the effect of annealing on the extent of solute crystallization was quantified.

MATERIALS AND METHODS

Materials

Disodium hydrogen phosphate (Na_2HPO_4) and monosodium dihydrogen phosphate (NaH_2PO_4) were obtained from Sigma, and were used without further purification. In all experiments deionized water was utilized. A pH meter (Oakton) was calibrated with standard buffer solutions (Oakton standard buffers; pH 10.00, 7.00 and 4.01; certified by NIST).

Preparation of Sodium Phosphate Buffer Solutions

Stock solutions of Na_2HPO_4 and NaH_2PO_4 were prepared at concentrations of 100, 20 and 10 mM and were mixed at the appropriate ratio to achieve a pH of 7.40 ± 0.02, diluted with water if necessary, to obtain 1, 8, 10, 20, 50 and 100 mM buffer solutions (31). The solutions were filtered (45 μm nylon filter), and stored in tightly closed scintillation vials in dark, at RT.

Methods

Laboratory Based X-ray Diffractometry

A powder X-ray diffractometer (Model XDS 2000, Scintag; Bragg-Brentano focusing geometry) with a variable temperature stage (High-Tran Cooling System, Micristar, Model 828D, R.G. Hansen & Associates; working temperature range: −190 to 300°C) and High-Purity Germanium solid-state detector was utilized for low-temperature studies. The buffer solution (200 μl) was pipetted into a copper sample holder, covered with a beryllium window, and cooled at 2°C/min, from room temperature to −50°C and held for 15 min. It was then exposed to CuKα radiation (45 kV × 40 mA) and the XRD patterns were obtained by scanning over the angular range of 2 to 45°2θ with a step size of 0.05° and a dwell time of 1 s.

Synchrotron XRD (Transmission Mode)

The experiments were performed at the synchrotron X-ray beamline 6-IDB (of MUCAT, sector 6) at the Advanced Photon Source, Argonne National Laboratory (Argonne, IL, USA). The variable temperature stage (High-Tran Cooling System, Micristar, Model 828D, temperature range: −190 to 300°C) was attached to a cradle (Eulerian 512) using an aluminum plate. A monochromatic X-ray beam (0.765338 Å; beam size 100 (vertical) × 200 (horizontal) μm) was used wherein only the channel cut triple-bounce of Si single crystal monochromator with [111] face polished, limited the line broadening to the theoretical limit, i.e., its Darwin width.

The flux of the incident X-rays (intensity: 10^{13} photons/s/mrad^2/mm^2) was attenuated to prevent detector saturation. An image plate 2D surface area detector (MAR3450) with 3,450 × 3,450 pixel resolution in 34.5 mm diameter area with readout time of 108 s (best resolution mode) was used. The sample-to-detector distance was maintained at 526.41 mm. The calibration was performed using a silicon standard (SRM

640b, NIST). The time-resolved 2D data was integrated to 1D *d*-spacing or 2θ scans using the FIT2D software developed by A. P. Hammersley of the European Synchrotron Radiation Facility (32,33). A commercial software package was used for determining the integrated peak intensities (JADE, version 7.1, Materials Data, Inc.).

The buffer solution (200 µl) was placed in a specially designed Al sample cell with a Kapton® window. The entire setup was covered with a beryllium window. The solutions were cooled at 2°C/min from room temperature to −50°C and held for 15 min. The frozen solutions were exposed to high-intensity X-ray beam (exposure time of 5 or 10 s) at different time intervals. Additionally, *blank* data were obtained by exposing the sample cell without buffer solution. In selected instances, after cooling the solutions to −50°C, they were heated to −20°C at 2°C/min and annealed for 5–10 min.

RESULTS AND DISCUSSIONS

Laboratory XRD

The crystallization of DHPD from phosphate buffer solutions, with initial concentrations of 50 and 100 mM, was readily evident when the solutions were cooled to −50°C. The peak with *d*-spacing of 5.40 Å was unique to DHPD, while crystalline ice was characterized by lines with *d*-spacings of 3.93, 3.65, 3.46 and 2.68 Å (Fig. 1). Earlier, we had demonstrated buffer salt crystallization when the initial buffer concentration was ≥190 mM (24,25).

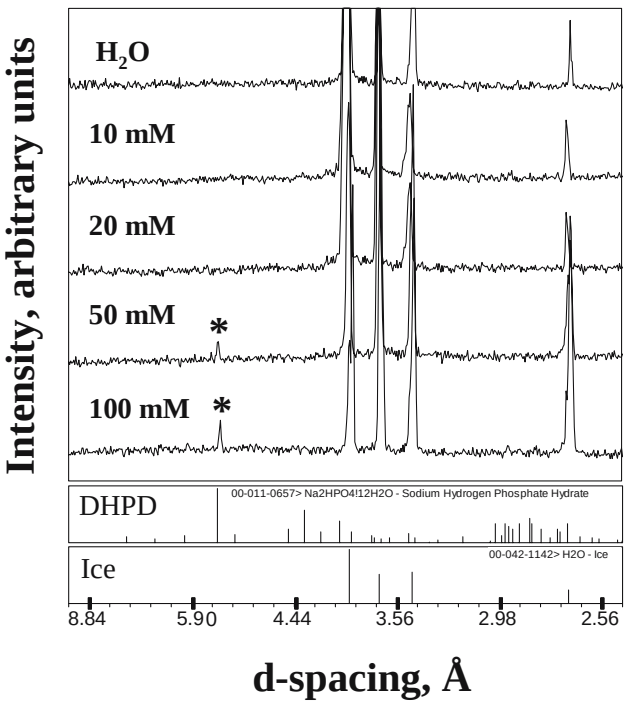

Fig. 1. XRD patterns, obtained using the laboratory source, of frozen sodium phosphate buffer (Na_2HPO_4 + NaH_2PO_4) solutions, with initial concentration ranging from 10 to 100 mM. All the solutions, with initial pH of 7.4, were cooled from RT to −50°C at 2°C/min, and the XRD patterns were obtained. For comparison purposes, the stick patterns of ice (34) and DHPD (35) are provided. *Diagnostic peak of disodium hydrogen phosphate dodecahydrate (DHPD; Na_2HPO_4•$12H_2O$) at 5.40 Å.

Gomez *et al.*, based on shift in solution pH, had suggested crystallization of DHPD even at a low initial buffer concentration of 8 mM (18,19). The absence of the characteristic peak of DHPD, at initial buffer concentrations of 10 and 20 mM (Fig. 1), might be either due to kinetic factors or the lack of sensitivity of the laboratory based XRD method (18,19,29). Another potential problem with the laboratory based XRD method is that the identification of crystalline DHPD was based on a single peak. In multi-component formulations, the detection of DHPD can be challenging in the presence of other crystalline formulation components, with *d*-spacings in the vicinity of 5.4 Å. Both of these problems could be overcome with the use of synchrotron radiation.

Synchrotron XRD

Figure 2 contains the 2D and 1D SXRD patterns of 100 mM buffer solutions. For comparison purposes, the XRD pattern obtained from the laboratory source has also been presented (Panel B). The diffraction lines with *d*-spacings of 5.42, 4.49, 4.30, 4.15, 3.99, 2.95, 2.90, 2.86, 2.82 Å are unique to DHPD, while the hexagonal ice is characterized by the 3.93, 3.65, 3.46 and 2.68 Å lines (Panel A).

While almost all the characteristic lines of DHPD were present in the SXRD pattern, the laboratory source revealed only one diagnostic peak at 5.4 Å. In addition, there was a pronounced improvement (>10-fold) in the signal-to-noise ratio (s/n), as determined for the 5.4 Å line (100 mM). From a s/n value of ~4 for the laboratory source, it increased to 61, when synchrotron radiation was used.

Crystallization from Buffer Solutions in the 1–10 mM Range

Crystallization of DHPD was readily evident from buffer solutions of 10 and 8 mM initial concentrations (Fig. 3, Panels A and B), based on the characteristic lines with *d*-spacings of 5.42, 4.30, 2.86 and 2.82 Å. When the concentration was reduced to 1 mM, the crystallization of the buffer salt was evident based on the appearance of the most intense 4.30 Å line (Panel C). In all cases, the presence of ice was confirmed by the 3.93, 3.65, 3.46 and 2.68 Å lines.

Solute Crystallization–Effect of Annealing

Since selective crystallization of DHPD causes a significant pH shift in the freeze-concentrate, it is of interest to identify the extent of its crystallization both during cooling and during annealing. The buffer solution (10 or 100 mM) was first cooled to −50°C at 2°C/min, held for 15 min, then heated to −20°C at 2°C/min, and annealed for 10 min. From the 2D-SXRD patterns, the crystallization appears to be complete by the time the solution is cooled to −50°C (Fig. 4). The integrated intensities of several lines of DHPD formed the basis for quantification of crystalline DHPD in the frozen solution. Based either on the intensity of single lines, or the sum of the intensities of several lines, it was confirmed that there was no increase in the crystalline DHPD content following anneal-

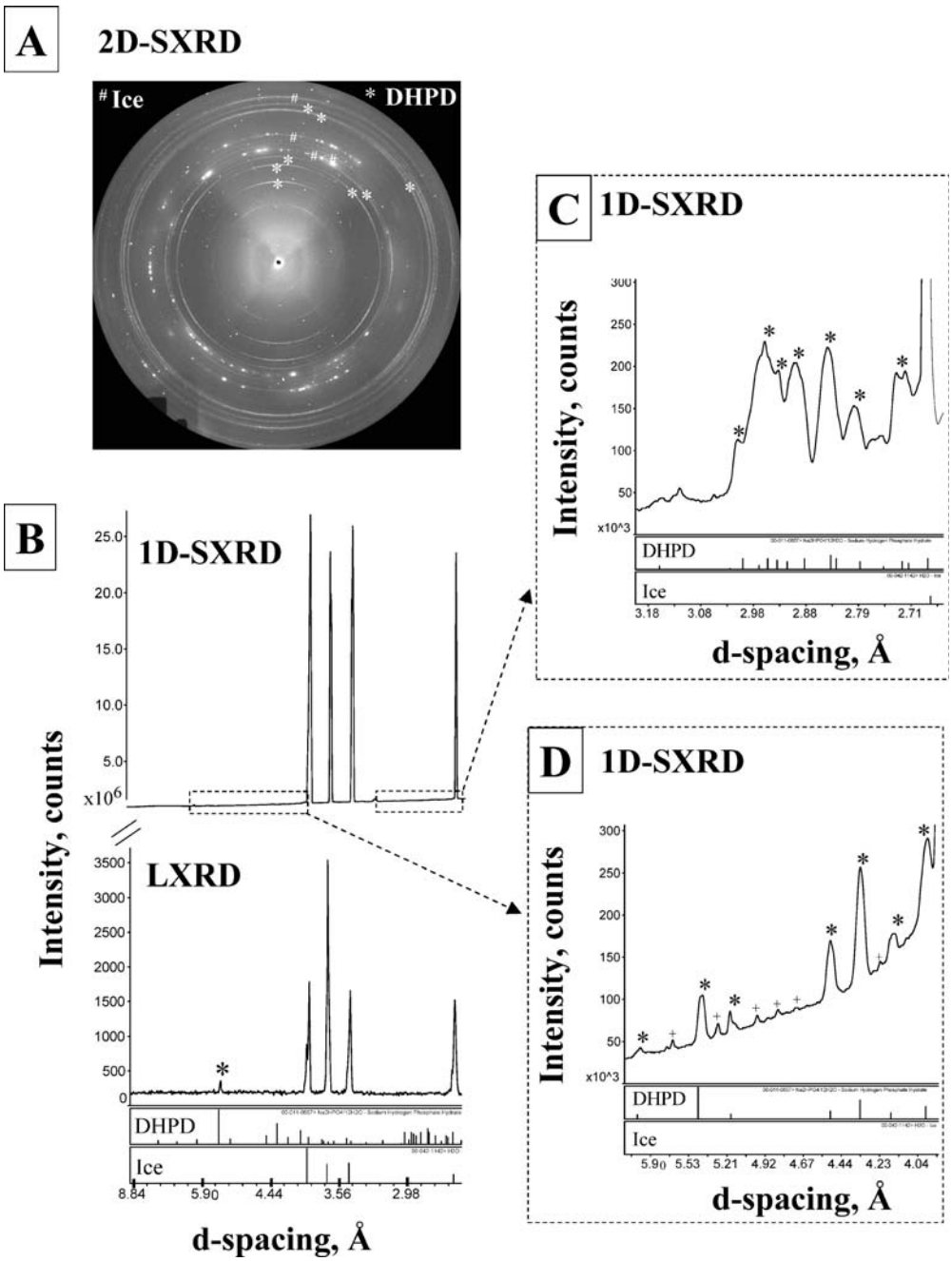

Fig. 2. Synchrotron XRD patterns of frozen sodium phosphate buffer solution (initial concentration: 100 mM; pH: 7.4). (A) 2D-SXRD. (B) 1D-SXRD. For comparison purposes, the XRD pattern obtained using the laboratory source (*LXRD*) is also provided. (C), (D) Selected regions of the 1D-SXRD pattern have been expanded to visualize several diagnostic peaks of $Na_2HPO_4 \cdot 12H_2O$ (*). The buffer solutions were cooled from RT to −50°C at 2°C/min. #*Diagnostic diffraction lines* corresponding to *hexagonal ice*. +Multiple reflection peaks due to Al-sample cell used in the experiment.

ing (Fig. 5). Thus the crystallization appears to be complete in the solution cooled to −50°C.

SIGNIFICANCE

The detection of crystalline DHPD, from a 1 mM buffers solution, was a significant improvement in sensitivity compared to previous approaches either utilizing laboratory XRD (crystallization from a 190 mM buffer solution) or based on pH shift (8 mM buffer solution) (18,19). *This provides, for the first time, direct evidence of buffer crystallization in frozen solutions even when the initial phosphate buffer concentration is as low as 1 mM.* Since numerous diagnostic peaks of DHPD were observed, the detection is unambiguous and reliable.

It is widely reported that only disodium hydrogen phosphate dodecahydrate (DHPD) crystallizes from frozen solutions (15–25). High sensitivity of the SXRD enabled us to

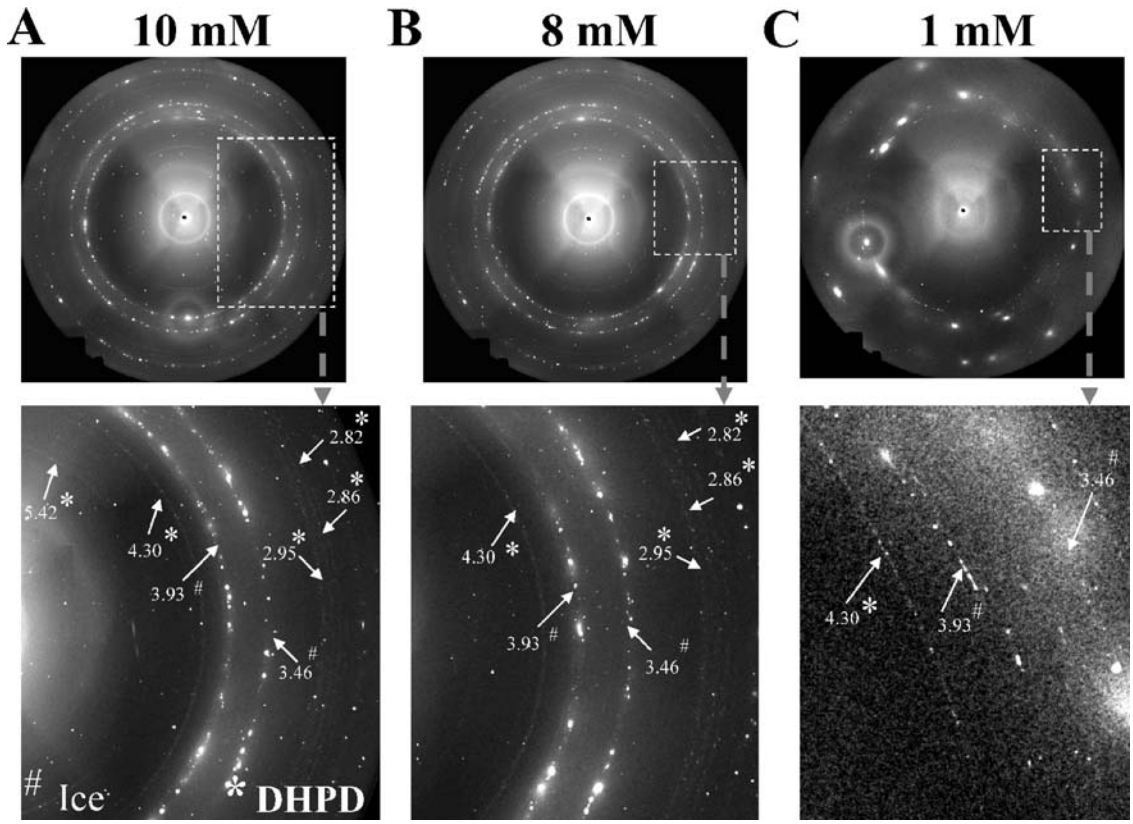

Fig. 3. Synchrotron 2D-XRD patterns of frozen sodium phosphate buffer solutions, with initial concentration ranging from 1 to 10 mM (pH = 7.4 at RT). (A) 10 mM. (B) 8 mM. (C) 1 mM. Selected regions have been expanded to reveal the *diagnostic lines* of DHPD (*). Some characteristic lines of *hexagonal ice* (#) are also pointed out. The buffer solutions were cooled from RT to −50°C at 2°C/min.

rule out the crystallization of any other phases of disodium hydrogen phosphate and monosodium dihydrogen phosphate (36–38). The SXRD patterns, over the concentration range of 1–100 mM, were compared with the published International Centre for Diffraction data (ICDD) card patterns of $Na_2HPO_4 \cdot xH_2O$ and $NaH_2PO_4 \cdot xH_2O$ (where x = 0 to 7). Both before and after annealing, only $Na_2HPO_4 \cdot 12H_2O$ was detected. Thus, only the most insoluble salt, $Na_2HPO_4 \cdot 12H_2O$, crystallized spontaneously following the ice crystallization. Additionally, since crystalline monosodium dihydrogen phosphate was not detected, its existence in the amorphous phase was confirmed.

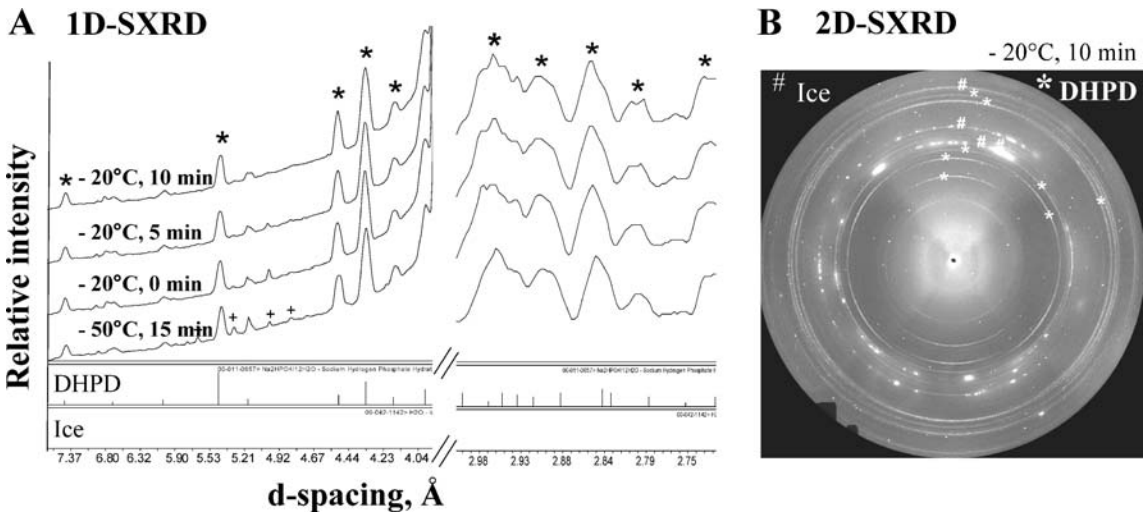

Fig. 4. Synchrotron XRD patterns of sodium phosphate buffer solution (initial concentration: 100 mM, pH: 7.4) at different stages of freezing and annealing: (A) 1D-SXRD. (B) 2D-SXRD pattern after annealing. The buffer solutions were cooled from RT to −50°C at 2°C/min and held for 15 min. It was then heated to −20°C at 2°C/min and annealed for 10 min. Some *diagnostic lines* corresponding to $Na_2HPO_4 \cdot 12H_2O$ (*) and *hexagonal ice* (#) are displayed. Also, multiple reflection peaks (+) due to Al-sample cell are shown.

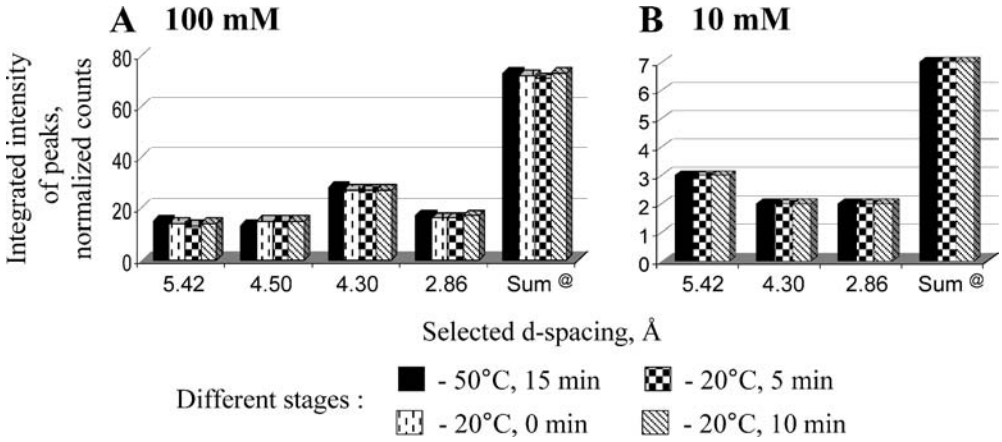

Fig. 5. Histograms displaying the integrated intensities of several characteristic peaks of DHPD at different stages of freezing and annealing. The initial buffer concentrations were: (A) 100 mM and (B) 10 mM. [@]Sum of the integrated intensities of the peaks with *d*-spacing of 5.42, 4.50 (only for 100 mM buffer solution), 4.30 and 2.86 Å.

Solute crystallization is usually facilitated by annealing the frozen solution. In our system, the crystallization appeared to be complete during freezing, and annealing did not increase the concentration of crystalline DHPD in the frozen solution (Fig. 5). However, in other buffer systems, for example monosodium succinate has a propensity to crystallize during annealing (6). In such systems, the change in the concentration of the crystalline phase, at different stages of freezing, and as a function of annealing time and temperature can be quantified (analogous to Fig. 5). This can provide an indirect measure of the change in pH of the freeze-concentrate due to selective crystallization of buffer salt.

While the phosphate buffer is a model system, the SXRD can be utilized to detect solute crystallization, and specifically the crystallization of other buffer salts of pharmaceutical interest. This technique is particularly suited for the characterization of multi-component systems with several crystalline phases. Moreover, the entire freeze-drying cycle can be carried out in the sample chamber, and phase transitions during each stage of the process, can be monitored. Thus high sensitivity of the SXRD, coupled with the *in situ* freeze-drying technique, can enable the development of robust freeze-dried formulations. We are currently investigating the utility of SXRD to study such systems, and specifically protein formulations.

CONCLUSIONS

Sensitivity of the synchrotron XRD, for the detection of solute crystallization in frozen systems was established, using sodium phosphate buffer as the model system. Crystallization of disodium hydrogen phosphate dodecahydrate (DHPD) was detected in buffer solutions down to a concentration of 1 mM. The detection was often based on numerous diagnostic peaks of DHPD.

ACKNOWLEDGMENTS

The authors thank Dr. Douglas Robinson, Advanced Photon Source, Argonne National Laboratory for the beamline management and support during the experiments. This work was supported, in part, by a Research Challenge award from the Ohio Board of Regents. Use of the Advanced Photon Source (APS) was supported by the U.S. Department of Energy, Basic Energy Sciences, Office of Science, under Contract No. W-31-109-Eng-38. The Midwest Universities Collaborative Access Team (MUCAT) sector at the APS is supported by the U.S. Department of Energy, Basic Energy Sciences, Office of Science, through the Ames Laboratory under Contract No. W-7405-Eng-82. We thank Linda Sauer for her assistance in setting up the instrumentation.

REFERENCES

1. X. Tang and M. J. Pikal. Design of freeze-drying processes for pharmaceuticals: practical advice. *Pharm. Res.* **21**:191–200 (2004).
2. L. A. Trissel. *Handbook of Injectable Drugs*, ASHP, Bethesda, MD, 1994.
3. T. W. Randolph. Phase separation of excipients during lyophilization: effects on protein stability. *J. Pharm. Sci.* **86**:1198–1202 (1997).
4. M. J. Pikal. Freeze Drying. *Encyclopedia of Pharmaceutical Technology*, Marcel Dekker, Inc. p.1299–1326, (2002).
5. E. Y. Shalaev, F. Franks, and P. Echlin. Crystalline and amorphous phases in the ternary system water-sucrose-sodium chloride. *J. Phys. Chem.* **100**:1144–1152 (1996).
6. E. Y. Shalaev. The impact of buffer on processing and stability of freeze-dried dosage forms, part 1: solution freezing behavior. *American Pharm. Rev.* **8**:80–87 (2005).
7. R. G. Bates. *Determination of pH. Theory and Practice*. 2nd ed. John Wiley & Sons, New York, 1973, p. 90., .
8. K. A. Pikal-Cleland, J. L. Cleland, T. J. Anchordoquy, and J. F. Carpenter. Effect of glycine on pH changes and protein stability during freeze-thawing in phosphate buffer systems. *J. Pharm. Sci.* **91**:1969–1979 (2002).
9. M. J. Pikal, K. M. Dellerman, M. L. Roy, and R. M. Riggin. The effect of formulation variables on the stability of freeze-dried human growth harmone. *Pharm. Res.* **8**:427–436 (1991).
10. S. S. Larsen. Studies on stability of drugs in frozen systems. IV. The stability of benzylpenicillin sodium in frozen aqueous solutions. *Dansk Tidsskr. Farm.* **45**:307–316 (1971).
11. M. P. W. M. te Booy, R. A. de Ruiter, and A. L. J. de Meere. Evaluation of the physical stability of freeze-dried sucrose-

containing formulations by differential scanning calorimetry. *Pharm. Res.* **9**:109–114 (1992).
12. M. J. Akers, N. Milton, S. R. Byrn, and S. L. Nail. Glycine crystallization during freezing: the effects of salt form, pH, and ionic strength. *Pharm. Res.* **12**:1457–1461 (1995).
13. A. Pyne and R. Suryanarayanan. Phase transitions of glycine in frozen aqueous solutions and during freeze-drying. *Pharm. Res.* **18**:1448–1454 (2001).
14. S. S. Larsen. Studies on stability of drugs in frozen systems. VI. The effect of freezing on pH for buffered aqueous solutions. *Arch. Pharm. Chemi Sci. Ed.* **1**:41–53 (1973).
15. L. van den Berg. pH changes in buffers and foods during freezing and subsequent storage. *Cryobiology* **3**:236–242 (1966).
16. L. van den Berg and D. Rose. Effect of freezing on the pH and composition of sodium and potassium phosphate solutions: the reciprocal system: KH_2PO_4–Na_2HPO_4–H_2O. *Arch. Biochim. Biophys.* **81**:319–329 (1959).
17. L. van den Berg and D. Rose. The effect of addition of sodium and potassium chloride to the reciprocal system: KH_2PO_4–Na_2HPO_4–H_2O on pH and composition during freezing. *Arch. Biochim. Biophys.* **84**:305–315 (1959).
18. G. Gomez, M. J. Pikal, and N. Rodriguez-Hornedo. Effect of initial buffer composition on pH changes during far-from equilibrium freezing of sodium phosphate buffer solutions. *Pharm. Res.* **18**:90–97 (2001).
19. G. Gomez. *Crystallization-related pH changes during freezing of sodium phosphate buffer solutions,* Ph.D. Dissertation, University of Michigan, Ann Arbor, Michigan, 1995.
20. Y. Orii and M. Morita. Measurement of the pH of frozen buffer solutions by using pH indicators. *J. Biochem.* **81**:163–168 (1977).
21. B. S. Chang and C. S. Randall. Use of subambient thermal analysis to optimize protein lyophilization. *Cryobiology* **29** 632–656 (1992).
22. N. Murase and F. Franks. Salt precipitation during the freeze-concentration of phosphate buffer solutions. *Biophys. Chem.* **34**:293–300 (1989).
23. N. Murase, P. Echlin, and F. Franks. The structural states freeze-concentrated and freeze-dried phosphates studied by scanning electron-microscopy and differential scanning calorimetry. *Cryobiology* **28**:364–375 (1991).
24. R. K. Cavatur and R. Suryanarayanan. Characterization of frozen aqueous solutions by low temperature X-ray powder diffractometry. *Pharm. Res.* **15**:194–199 (1998).
25. A. Pyne, K. Chatterjee, and R. Suryanarayanan. Crystalline to amorphous transition of disodium hydrogen phosphate during primary drying. *Pharm. Res.* **20**:802–803 (2003).
26. N. Blagden, R. Davey, M. Song, M. Quayle, S. Clark, D. Taylor, and A. Nield. A novel batch cooling crystallization for *in situ* monitoring of solution crystallization using energy dispersive X-ray diffraction. *Cryst. Growth Design***3**:197–201 (2003).
27. R. Surana and R. Suryanarayanan. Quantitation of crystallinity in substantially amorphous pharmaceuticals and study of crystallization kinetics by X-ray powder diffractometry. *Powder Diffr.* **15**:2–6 (2000).
28. C. Nunes, R. Suryanarayanan, C. E. Botez, and P. W. Stephens. Characterization and crystal structure of *d*-mannitol hemihydrate. *J. Pharm. Sci.* **93**:2800–2809 (2004).
29. C. Nunes. *Use of High-Intensity X-Radiation in Solid-State Characterization of Pharmaceuticals*, Ph.D. Dissertation, Department of Pharmaceutics, University of Minnesota, 2005.
30. C. Nunes, A. Mahendrasingam, and R. Suryanarayanan. Quantification of crystallinity in substantially amorphous materials by synchrotron X-ray powder diffractometry. *Pharm. Res.* **22**: 1942–1953 (2005).
31. C. Mohan. Buffers: a guide for the preparation and use of buffers in biological systems. Calbiochem®, EMD Biosciences, Inc. 2003.
32. A. P. Hammersley. *ESRF internal report*, **ESRF97HA02T**, "Fit2D: an introduction and overview," (1997).
33. A. P. Hammersley, S. O. Svensson, M. Hanfland, A. N. Fitch, and D. Häusermann. Two-dimensional detector software: from real detector to idealized image or two-theta scan. *High Press. Res.* **14**:235–248 (1996).
34. Powder Diffraction File. (hexagonal ice: PDF-2, Card #00-042-1142), International Centre for Diffraction Data, Newtown Square, PA, 1996.
35. Powder Diffraction File. (disodium hydrogen phosphate dodecahydrate: PDF-2, Card #00-011-0657), International Centre for Diffraction Data, Newtown Square, PA, 1996.
36. D. H. Templeton, H. W. Ruben, and A. Zalkin. Entropy and crystal structure of hydrates of disodium hydrogen phosphate. *J. Phys. Chem.* **94**:7830–7834 (1990).
37. A. Ghule, C. Bhongale, and H. Chang. Monitoring dehydration and condensation processes of Na_2HPO_4•$12H_2O$ using thermo-Raman spectroscopy. *Spectrochim. Acta, Part A: Mol. Biomol. Spectrosc.* **59A**(7): 1529–1539 (2003).
38. Powder Diffraction File. (crystalline phases of disodium hydrogen phosphate and monosodium dihydrogen phosphate, Na_2HPO_4•$7H_2O$: PDF-2, Card #00-010-0191; NaH_2PO_4•$2H_2O$: PDF-2, Card #00-010-0198; NaH_2PO_4•H_2O: PDF-2, Card #00-011-0651; NaH_2PO_4: PDF-2, Card #00-011-0659), International Centre for Diffraction Data, Newtown Square, PA, 1996.